Received: 29 April 2020 | Revised: 3 June 2020 | Accepted: 15 June 2020

DOI: 10.1096/fj.202001062R

RESEARCH ARTICLE

THE FASEB JOURNAL

Network determinants of cardiovascular calcification and repositioned drug treatments

Jun-Seop Song[1] | Rui-Sheng Wang[1] | Jane A. Leopold[2] | Joseph Loscalzo[1]

[1]Department of Medicine, Brigham and Women's Hospital, Harvard Medical School, Boston, MA, USA

[2]Division of Cardiovascular Medicine, Brigham and Women's Hospital, Harvard Medical School, Boston, MA, USA

Correspondence
Joseph Loscalzo, Department of Medicine, Brigham and Women's Hospital, Harvard Medical School, 75 Francis Street, Boston, MA 02115, USA.
Email: jloscalzo@rics.bwh.harvard.edu

Funding information
National Heart, Lung, and Blood Institute (NHLBI), Grant/Award Number: HG007690, HL108630, HL119145 and HL125215; American Heart Association (AHA), Grant/Award Number: D700382 and 19AIML34980000

Abstract

Ectopic cardiovascular calcification is a highly prevalent pathology for which there are no effective novel or repurposed pharmacotherapeutics to prevent disease progression. We created a human calcification endophenotype module (ie, the "calcificasome") by mapping vascular calcification genes (proteins) to the human vascular smooth muscle-specific protein-protein interactome (218 nodes and 632 edges, $P < 10^{-5}$). Network proximity analysis was used to demonstrate that the calcificasome overlapped significantly with endophenotype modules governing inflammation, thrombosis, and fibrosis in the human interactome ($P < 0.001$). A network-based drug repurposing analysis further revealed that everolimus, temsirolimus, and pomalidomide are predicted to target the calcificasome. The efficacy of these agents in limiting calcification was confirmed experimentally by treating human coronary artery smooth muscle cells in an in vitro calcification assay. Each of the drugs affected expression or activity of their predicted target in the network, and decreased calcification significantly ($P < 0.009$). An integrated network analytical approach identified novel mediators of ectopic cardiovascular calcification and biologically plausible candidate drugs that could be repurposed to target calcification. This methodological framework for drug repurposing has broad applicability to other diseases.

KEYWORDS

blood vessel, calcification, protein interaction, smooth muscle cell, therapeutics

1 | INTRODUCTION

Ectopic cardiovascular calcification is a highly prevalent end-pathophenotype that is associated with increasing age, diabetes mellitus, atherosclerosis, and chronic kidney disease (CKD).[1] When present, this pathological finding portends an increased risk for cardiovascular morbidity and mortality.[2-4] The mechanisms underlying cardiovascular calcification are multifactorial and include osteoblastic differentiation of vascular smooth muscle cells (VSMC) in

Abbreviations: ARVD, arrhythmogenic right ventricular dysplasia; ATC, anatomical therapeutic chemical; CKD, chronic kidney disease; GWAS, genome-wide association study; HCSMC, human coronary artery smooth muscle cell; IL6, interleukin 6; LCC, largest connected component; mTOR, mammalian target of rapamycin; NFE2L2, nuclear factor erythroid-derived 2-like 2 (also known as NRF2); PCOS, polycystic ovary syndrome; PPI, protein-protein interaction; rhBMP-2, recombinant human bone morphogenetic protein-2; T2DM, type 2 diabetes mellitus; VSMC, vascular smooth muscle cell.

situ, release of pro-calcifying extracellular matrix vesicles, dysregulation of mineral homeostasis, and inflammation, among others.[1,5] These calcification processes have been identified in complex cardiovascular diseases, such as atherosclerosis,[6] aortic valve stenosis,[7] and aortic aneurysm,[8] that are characterized by calcification as well as inflammation, fibrosis, and thrombosis.[9] This suggests that these four endophenotypes (ie, calcification, inflammation, fibrosis, and thrombosis) may be pathologically linked to each other and, thereby, all play an intermediate role in the development of complex cardiovascular diseases.[10-13] Evidence to support this concept was demonstrated by Ghiassian and colleagues using molecular network analysis.[13] They showed that the inflammation, fibrosis, and thrombosis molecular subnetworks clustered significantly and overlapped highly with each other in the human protein-protein interaction (PPI) network, and that these subnetworks are enriched with cardiovascular disease-associated genes.[13] Whether the calcification endophenotype associates mechanistically with complex diseases independently or dependently of these other endophenotypes has not been studied systematically. Furthermore, despite our mechanistic understanding of the molecular and cellular events that promote ectopic calcification, there are no available pharmacotherapies that inhibit the development of cardiovascular calcification, which is likely attributable to its complex pathobiology.

Recently, network analysis-based computational methods have emerged as novel tools for identifying previously unknown functional relationships between drug targets and diseases[14,15] or between different diseases[16,17] in the PPI network. These network-based techniques arise from the simple biological observations that cellular components (genes or proteins) associated with a specific phenotype tend to interact locally with each other, clustering into a "disease module" in the PPI network.[18,19] Additionally, diseases with network modules that significantly overlap with those of other diseases show an increased tendency to have similar clinical manifestations, pathological pathways, coexpression patterns, and comorbidities.[17,20] Several non-Euclidean network distance measures and topology-based centrality metrics have been developed to analyze the functional characteristics of disease modules in the PPI network.[15,21] Thus, mapping the genes (gene products) associated with obscure complex traits to the interactome potentially provides novel information on disease-disease relationships or disease-drug relationships, which are not available from conventional genome-wide association study (GWAS) or linear model-based clinical/epidemiological analyses. The network-based drug repurposing approach has been used successfully to discover novel drug candidates for coronary artery disease,[14] lung adenocarcinoma,[22] pulmonary arterial hypertension, and COVID-19,[23,24] as well as to predict the efficacy of drug combinations.[25] This drug repositioning framework also provides new mechanistic insights into approved drugs with well-established pharmacological features, facilitating the discovery of drug candidates for complex traits with maximal efficacy and minimal toxicity.

In this study, we define a functional module for vascular smooth muscle cell (VSMC) calcification in the human VSMC-specific interactome and utilize this module and its localization in the PPI network to determine the relationship between the calcification endophenotype and other endophenotypes to cardiovascular disease. We then evaluate potential pathobiological similarities with other general diseases using the PPI network. Finally, we screen drug candidates for effects on vascular calcification using a network-based drug repurposing framework and provide an in vitro correlate to validate this approach.

2 | MATERIALS AND METHODS

2.1 | Building a human PPI network

The comprehensive human PPI network was built by integrating 18 public resources with multiple interaction types: (1) binary PPIs identified by high-throughput yeast-two-hybrid systems as well as high-quality PPIs from the Center for Cancer Systems Biology (CCSB) Human Interactome,[26-32] (2) protein complexes tested by three-dimensional protein structure determinations or affinity-purification mass spectrometry,[33-39] (3) kinase-substrate interactions,[40,41] and (4) high-quality literature-based signaling pathways.[42,43] The resulting human interactome included 15 849 proteins (nodes) and 188 973 interactions (edges).

2.2 | The vascular smooth muscle cell-specific interactome

To identify the functional endophenotype module in the VSMC-specific interactome, we used a microarray data set (GeneChip Human Gene 2.0 ST Array) from human pulmonary arterial smooth muscle cells.[44] The microarray data set covered 24 838 Entrez genes, of which 15 026 genes were also represented in our PPI network (94.8% coverage). The probe sets were flagged as "present" or "absent" using a detection-above-background (DABG) threshold of 0.01. Genes identified as "present" that are included in the human PPI network were used to construct the VSMC-specific interactome. The VSMC-specific interactome constructed in this way contained 11 129 proteins sharing 135 754 interactions.

2.3 | Collecting vascular calcification and other relevant endophenotype genes

We obtained 330 seed genes from Human GeneCards (http://www.genecards.org, accessed at Dec 27, 2018) with the search term, "vascular calcification." Additionally, we manually retrieved 303 seed genes by reviewing PubMed articles with the search term, "vascular calcification." A total of 279 of 505 seed genes were mapped to the VSMC-specific interactome (Supplementary Table 1).

A functional vascular calcification module in the VSMC-specific interactome was identified as the largest connected component (LCC) in the module. The statistical significance of the LCC is calculated by comparing the observed LCC size with an LCC comprised of a set of randomly selected nodes of the same size obtained from 1000 repetitions. A z-score was calculated as $z = \frac{\mathrm{LCC}_{\mathrm{observed}} - \langle \mathrm{LCC} \rangle_{\mathrm{randomized}}}{\sigma_{\mathrm{randomized}}}$ where $\langle \mathrm{LCC} \rangle_{\mathrm{randomized}}$ and $\sigma_{\mathrm{randomized}}$ are the mean and SD of the randomized LCC distribution, respectively.

Additionally, inflammation, fibrosis, and thrombosis endophenotype seed genes/gene products (with at least two publications that provide independent, supportive evidence) were retrieved from Phenopedia (v5.4, https://phgkb.cdc.gov/PHGKB/startPagePhenoPedia.action). After mapping the endophenotype seed genes/gene products to the comprehensive human PPI network, endophenotype modules were defined as the LCC of the subnetworks induced by endophenotype seeds (Supplementary Table 1).[13] All endophenotype modules were constructed from the human PPI network, and were statistically clustered ($P < 10^{-5}$, permutation test).

2.4 | Evaluating disease-disease associations using a network distance measure

Associations between the vascular calcification endophenotype module and other human disease modules were evaluated in terms of the average network (non-Euclidean) distance. Disease genes were curated from PheGenI (https://www.ncbi.nlm.nih.gov/gap/phegeni, accessed at June 05, 2019) and OMIM (https://omim.org, accessed at June 05, 2019) databases and combined using the hierarchical structure of the MeSH classification (v.2019) as previously described by Menche and colleagues.[17] After filtering out diseases with less than 20 genes or MeSH classification level less than 3, 266 different diseases with associated genes were obtained. Disease classes that have exactly the same gene sets were manually excluded.

The average shortest distance between the calcification module and the other disease modules in the entire human PPI network was calculated as $d_s(S,T) = \frac{1}{\|T\|} \sum_{t \in T} \frac{1}{\|S\|} \sum_{s \in S} d(s,t)$, where S is the protein set of the vascular calcification module, T is the set of disease proteins, and $d(s,t)$ is the shortest path length between nodes s and t in the PPI network.[45] To assess the statistical significance of the network distance between disease and drug targets, a randomized distance distribution corresponding to the expected distances between two randomly distributed nodes of the same size in a degree-preserving manner was generated. The randomized distance distribution was generated with over 1000 repetitions, and a z-score was calculated as $z = \frac{d_s(S,T) - \langle d \rangle_{\mathrm{randomized}}}{\sigma_{\mathrm{randomized}}}$ where $\langle d \rangle_{\mathrm{randomized}}$ and $\sigma_{\mathrm{randomized}}$ are the mean and SD of the randomized distance distribution, respectively. Assuming a normal distribution (Supplementary Figure 1), the Bonferroni-corrected P values < 0.01 were considered as statistically significant.

To determine whether disease module (D) is closer to a module (M) than another module (M'), the statistical significance for the distance difference was estimated. We assumed that $d_s(D,M)$ and $d_s(D,M')$ follow the normal distribution, $N(\mu, \sigma^2)$ and $N(\mu', \sigma'^2)$, respectively. Here, the mean and SD of the distribution can be estimated by generating a randomized distance distribution as described above. With this assumption of normality, $d_s(D,M) - d_s(D,M')$ is also normally distributed, $N(\mu - \mu', \sigma^2 + \sigma'^2)$; thus, we can compute a z-score for distance difference as $z = \frac{(d_s(D,M) - d_s(D,M')) - (\mu - \mu')}{\sqrt{\sigma^2 + \sigma'^2}}$. A $z < -1.0$ was used to identify differentially proximal disease modules. We denote this statistical framework as a "differential network proximity analysis."

2.5 | Generating the arrhythmogenic right ventricular dysplasia-specific interactome

The arrhythmogenic right ventricular dysplasia (ARVD)-specific interactome was constructed to explore the interactions between the calcification module and ARVD genes using publically available RNA-seq data from right ventricular tissue of patients with ARVD (n = 9, GEO accession number: GSE107475). Those genes with DESeq2-normalized counts ≥ cutoff value in >80% of samples were considered as ARVD-expressed genes.[14] The cutoff was set as the median value for all normalized counts across the nine samples; that is, approximately 50% of genes were used to construct the ARVD-specific interactome (10 248 nodes and 126 428 edges).

2.6 | Drug repurposing based on network proximity

Physical drug-target interactions of FDA-approved drugs were acquired from the DrugBank database (v5.1.2). Only human proteins included in the VSMC-specific interactome were considered. A total of 1068 drugs were included in the drug repurposing analysis.

Proximity between the vascular calcification module and drug targets in the VSMC-specific interactome was evaluated using the closest distance measure[14,15] defined as $d_c(S,T) = \frac{1}{\|T\|}\sum_{t \in T} min_{s \in S}\, d(s,t)$, where S is the protein set of the calcification module, T is the set of drug targets, and $d(s,t)$ is the shortest path length between nodes s and t in the VSMC-specific interactome. The z-score and P value were calculated by generating a reference distance distribution as described in the previous section. Drug candidates were identified using Bonferroni-corrected P values < 0.05. For each of the drugs, the drug targets-centered local subnetworks were generated by integrating all shortest paths of length less than four between the drug targets and key calcification genes, such as BMP2, RUNX2, SPP1, DNM1L, ENPP1, and TGFB1.

2.7 | Cell culture

Human coronary artery smooth muscle cells (HCSMC) (Lonza) were grown to confluence in SmBM medium (Lonza) supplemented with 5% fetal bovine serum, 0.2% human basic fibroblastic growth factor, 0.1% insulin, and 0.1% human epidermal growth factor without antibiotics at 37°C in 5% CO_2. Experiments were performed on cells from three separate donors at passages 3-5. For experiments, cells were exposed to calcification medium (β-glycerophosphate 10 mmol/L and ascorbic acid 50 nmol/L) for up to 10 days in the presence of everolimus (20 nmol/L),[46,47] pomalidomide (10 μmol/L),[48] or temsirolimus (10 nmol/L).[49] Medium was changed every 2 days.

2.8 | Western immunoblotting and densitometry

Cells were harvested and centrifuged at 1000 × g at 4°C for 5 minutes. The supernatant was discarded, and the pellets were frozen at −80°C. The pellet was homogenized, and 10-20 μg protein was added per lane. Proteins were size-fractionated electrophoretically using SDS-polyacrylamide gel electrophoresis and transferred to polyvinylidene fluoride membranes. After blocking for 1 hour with 5% of blocking buffer, the membranes were incubated with antibodies to CRBN (1:1000, Cell Signaling), p70S6K (1:1000, Cell Signaling), P-p70S6K (1:1000, Cell Signaling), mTOR (1:1000, Cell Signaling), P-mTOR (1:1000, Cell Signaling), or Runx2 (1:1000, abcam). Blots were visualized using the enhanced chemiluminescent system (Amersham Biosciences), stripped with Restore PLUS Western Blot Stripping Buffer (Thermo Scientific), and reprobed with GAPDH (1:2000 dilution, Cell Signaling) or actin (1:2000 dilution, Sigma) as a loading control. Densitometry was performed on immunoblots from a minimum of three experiments using Image Lab (BioRad) to quantitate band density.

2.9 | Alizarin red staining and quantification

Cells were washed twice with phosphate-buffered saline and fixed with 4% paraformaldehyde at 25°C for 15 minutes. The cells were then washed three times with distilled water, 2% Alizarin Red S solution (ScienCell) was added to each well, and the cells were incubated at 25°C for 30 minutes. The cells were then washed five times with distilled water and images were captured using a Canon PowerShot SD990 IS camera. After imaging, cells were stored at −20°C until assay. Cells were treated with 10% acetic acid, scraped from the plate, and heated to 85°C. After centrifugation, the supernatant was neutralized with 10% ammonium hydroxide, and absorbance was read at 405 nm on a SpectraMax 190 plate reader (Molecular Devices).

2.10 | Alkaline phosphatase activity

Alkaline phosphatase activity was measured using the Alkaline Phosphatase Assay kit (colorimetric) (abcam). Approximately 5×10^5 cells were homogenized in assay buffer and centrifuged at 15 000 rpm for 15 minutes at 4°C. The supernatant was incubated with p-nitrophenyl phosphate as a phosphatase substrate for 1 hour at 25°C. Dephosphorylation of the substrate was determined by reading the absorbance at 405 nm on a SpectraMax 190 plate reader (Molecular Devices).

2.11 | Cell proliferation and apoptosis

Cells proliferation was determined using the CellTiter 96 AQ_{ueous} One Solution Cell Proliferation Assay (Promega) according to the manufacturer's instructions. Briefly, the cells were incubated with tetrazolium compound [3-(4,5-dimethylthiazol-2-yl)-5-(3-carboxymethoxyphenyl)-2-(4-sulfophenyl)-2H-tetrazolium for 1 hour and the quantity of the formazan product was measured as the absorbance at 490 nm on a SpectraMax 190 plate reader (Molecular Devices). Apoptosis was assessed using the RealTime-Glo Annexin V Apoptosis Assay (Promega) according to the manufacturer's instructions. Luminescence over 30 minutes was read on a SpectraMax i3x Multimode plate reader (Molecular Devices). Data are reported at the maximal velocity (Vmax).

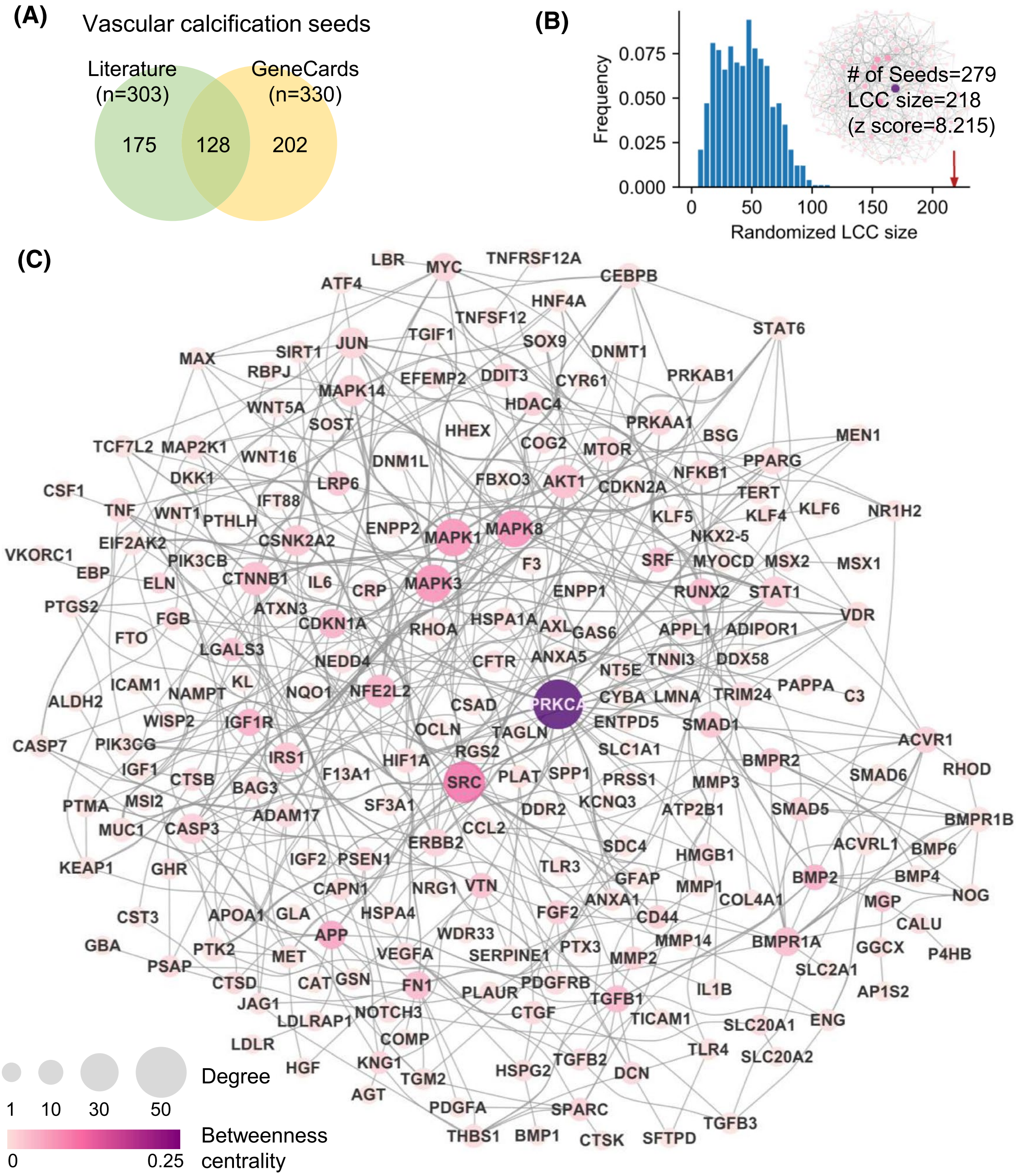

FIGURE 1 Identification of functional calcification endophenotype module ("calcificasome"). A, Vascular calcification-related seed genes were curated from PubMed and GeneCards. A total of 279 calcification seeds were mapped to the vascular smooth muscle cell-specific interactome. B, The largest connected component (LCC) of the calcification seeds is significantly larger than that expected by chance (P< 10−5). The randomized distribution of the LCC size is shown. C, The calcificasome is defined as the LCC of the calcification seeds (218 nodes and 632 edges). The node size and color indicate degree and betweenness centrality, respectively.

2.12 | Statistical analysis

Experimental data are presented as mean ± SEM. For comparison between treatment groups, the nonparametric Kruskal-Wallis test or Friedman test was performed with post hoc Dunn's multiple comparisons test were used. A $P < .05$ was considered significant. All analyses were performed using GraphPad Prism version 8.4.1 (La Jolla, CA).

3 | RESULTS

3.1 | Functional vascular calcification endophenotype module

We compiled a list of 505 vascular calcification-associated seed genes, 441 of which are present in the human PPI network (Figure 1A). To identify the functional vascular calcification module, we used microarray data from human

VSMC and constructed the VSMC-specific interactome. A total of 279 vascular calcification genes were mapped to the VSMC-specific interactome (Supplementary Table 1). We next defined a calcification endophenotype module (ie, "calcificasome") as the LCC of the subnetwork induced by the vascular calcification seeds (218 nodes and 632 edges, Figure 1B), which is significantly larger than that expected by chance ($P < 10^{-5}$, permutation test, Figure 1C).

3.2 | Relationship with other endophenotype and disease modules

To explore the pathobiology of the calcification process, we dissected the calcificasome endophenotype module by comparing it with other common endophenotype modules in cardiovascular diseases, such as the inflammasome, the fibrosome, and the thrombosome, on the whole human PPI network.[13] The calcificasome overlapped with the inflammasome, the fibrosome, and the thrombosome significantly greater than expected by chance in terms of the network proximity metric ($P < 0.001$). We identified 45 inflammasome-specific calcification genes (see Figure 2A), four fibrosome-specific calcification genes (ACVRL1, CTGF, CTSB, and TGFB3), four thrombosome-specific calcification genes (CALU, GGCX, KNG1, and MGP), and 19 genes associated with all four endophenotypes (AGT, CCL2, CRP, ICAM1, IL1B, IL6, LDLR, MMP1, MMP2, MMP3, NFE2L2, PPARG, PTGS2, SERPINE1, TGFB1, TLR4, TNF, VDR, and VEGFA).

We then generated three calcification subendophenotype modules defined as the LCC of genes shared between the calcificasome and each of the other three endophenotype modules, as well as the pure calcificasome defined as the LCC of the calcificasome-specific genes (Figure 2B). All four calcification subendophenotype modules were statistically significantly included in the calcificasome ($P < 10^{-5}$, permutation test). To discover the key intermediary proteins in the calcification process, we ranked all nodes by betweenness centrality (BC). We found that NFE2L2 (or NRF2) played a pivotal role not only in the original calcificasome (BC ranked 10th), but also in the inflammo-calcificasome, fibro-calcificasome, and thrombo-calcificasome (BC ranked 2nd, 1st, and 1st, respectively). In the pure calcificasome, MAPK3, BMPR1A, SMAD1, RUNX2, and BAG3 ranked as the top five BC nodes (see Supplementary Table 2 for a full list).

To determine potential pathological associations with other diseases, we evaluated disease-disease relationships by calculating the average shortest distance between calcification subendophenotype modules and other disease modules. A total of 86 of 266 diseases were associated with the pure calcificasome in terms of their network proximity ($P_{\text{adj}} < 0.01$, Supplementary Table 3). Seven diseases, including arrhythmogenic right ventricular dysplasia (ARVD), type 2 diabetes mellitus (DM), polycystic ovary syndrome (PCOS), and developmental bone diseases, were associated only with the pure calcificasome. In contrast, 18 diseases, including aortic aneurysm, cardiac arrhythmias, coronary artery disease, congenital heart defects, and inflammatory bowel diseases, were associated with all four calcification subendophenotype modules (see Figure 3A). For those diseases associated only with the pure calcificasome, we performed differential network proximity analysis to determine whether they are significantly closer to the pure calcificasome than to other subendophenotype modules (Figure 3B). ARVD was differentially associated with the pure calcificasome compared to the inflammo-calcificasome and thrombo-calcificasome ($z < -1.0$); however, the ARVD disease module is not significantly closer to the pure calcificasome than the fibro-calcificasome ($z \geq -1.0$).

We focused on ARVD to explore the potential mechanistic similarity between the calcification process and the pathobiology of ARVD. We generated an ARVD-interactome using RNA-seq data from the right ventricle of patients with ARVD ($n = 9$), and mapped the pure calcificasome to the ARVD-interactome (Figure 3C). ARVD genes, including DSG2, DSC2, PKP2, DSP, and JUP, formed a cluster in the ARVD-interactome connected to MYC, CSNK2A2, and BMPR1A, three genes known to be involved in the calcification process.

3.3 | Network-based in silico drug repurposing

Next, we performed in silico drug repurposing analysis for 1068 FDA-approved drugs by computing the network proximity[14] between the calcificasome and drug targets in the VSMC-specific interactome (Figure 4A). Filtering out non-oral/intravenous agents and cardiovascular drugs defined by first-level Anatomical Therapeutic Chemical (ATC) classification codes, we found six drugs whose targets are significantly more proximal to the calcificasome than that expected by chance ($P_{\text{adj}} < 0.05$, Table 1). To elucidate potential mechanisms of action, we further computed the network proximity between the targets of the six drug candidates and the calcification subendophenotype modules (Figure 4B). Everolimus and temsirolimus, which inhibit the activity of the mammalian target of rapamycin (mTOR) and siltuximab, which inhibits interleukin-6 (IL6), were significantly proximal to the inflammo-calcificasome. Pomalidomide, which inhibits CRBN, PTGS2, and TNF, proximally interacted with the inflammo-calcificasome, fibro-calcificasome, and thrombo-calcificasome. Only arsenic trioxide and dibotermin alfa were associated with the pure calcificasome.

Since arsenic trioxide has severe toxicity and dibotermin alfa (also known as recombinant human bone morphogenetic

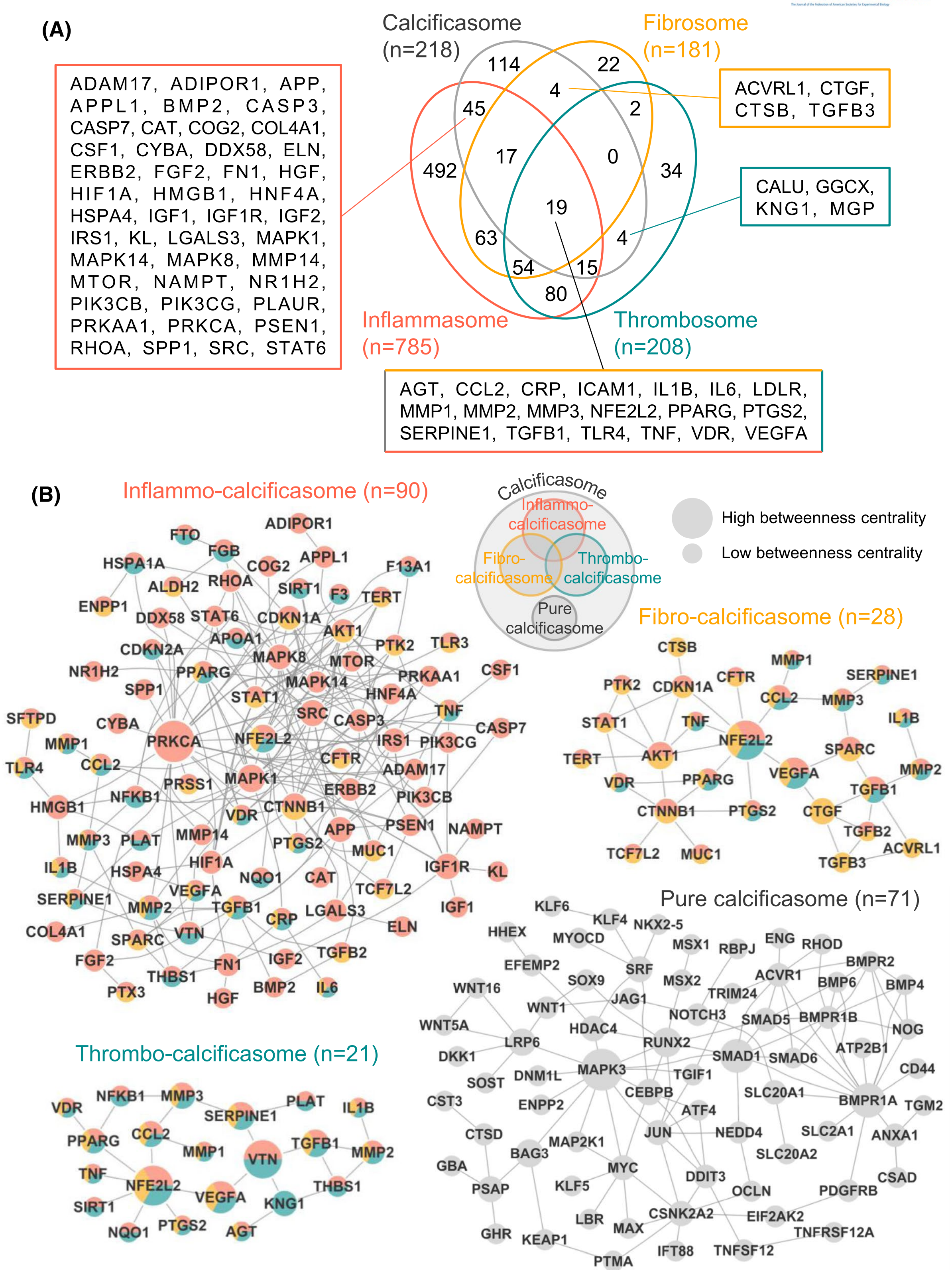

FIGURE 2 Relationships between the calcificasome and other endophenotype modules. A, Venn diagram of calcificasome (gray), inflammasome (red), fibrosome (orange), and thrombosome (blue). All endophenotype seed genes significantly formed the largest connected component on the PPI network ($P < 10^{-5}$). B, Calcification subendophenotype modules were significantly included in the calcificasome ($P < 10^{-5}$). The node size scale shows the betweenness centrality metric. The inflammasome, fibrosome, and thrombosome nodes are colored as red, orange, and blue, respectively.

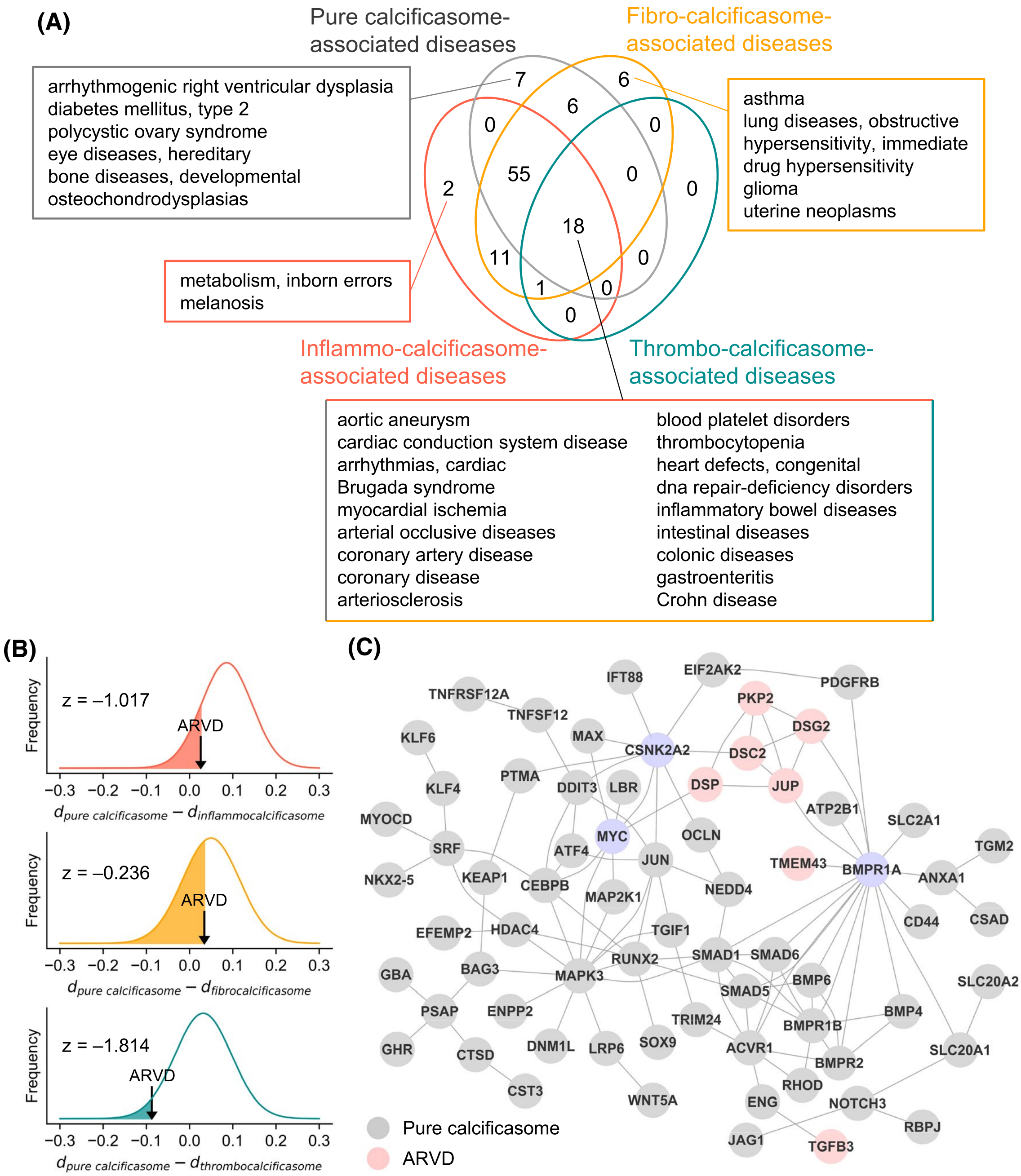

FIGURE 3 Disease associations of the calcification subendophenotype modules to untargeted complex diseases (n = 266) in terms of the average network distance on the PPI network. A, Diseases associated with the calcification subendophenotype modules are displayed ($P_{adj} < 0.01$). Seven diseases are specifically associated with the pure calcificasome ("abnormalities, multiple" are excluded due to the ambiguous disease classification). B, Differential network proximity analysis revealed that the arrhythmogenic right ventricular dysplasia (ARVD) module is significantly closer to the pure calcificasome than the inflammo-calcificasome or thrombo-calcificasome ($z < -1.0$). C, ARVD genes (red) are directly connected to the pure calcificasome genes (purple) in the ARVD-interactome

protein-2, rhBMP-2) actives a pro-calcification pathway (ie, BMP2), we excluded them for downstream in vitro analysis. We also excluded siltuximab because while IL6 has been implicated in VSMC calcification,[50] the IL6 receptor is only modestly expressed in VSMC. Therefore, we focused on everolimus, temsirolimus, and pomalidomide as potential drug candidates for inhibiting the calcification process. We further proposed potential anti-calcific mechanisms of action for these three drugs by generating local subnetworks, including all shortest paths between the drug targets and key calcification regulators (Figure 4C,D).

3.4 | In vitro experimental validation

To confirm the in silico analyses, human coronary artery smooth muscle cells (HCSMCs) were exposed to calcification medium for 10 days in the presence of everolimus

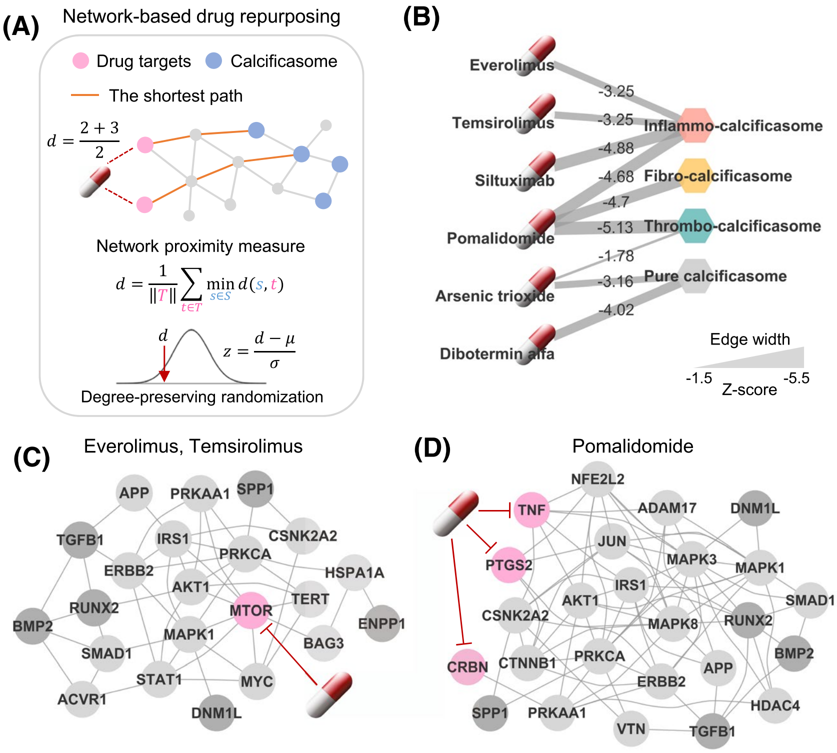

FIGURE 4 Network-based in silico drug repurposing for the calcificasome. A, A pipeline of the drug repurposing framework (computing the network proximity between drug targets and the calcificasome in the vascular smooth muscle cell-interactome). For each drug target (pink), the shortest path length from the drug target to the calcificasome proteins (blue) was measured and averaged. To evaluate the significance of the network proximity (d_c), the *z*-score was calculated by comparing the closest distance to a reference distribution of distances obtained from degree-preserving randomization. B, Association between six drug candidates and the calcification subendophenotype modules in terms of the network proximity measure. Only significant associations are displayed ($P < 0.05$). Edge width indicates a *z*-score for the network proximity. C and D, The drug targets (and inferred mechanisms-of-action) for everolimus/temsirolimus (C) and pomalidomide (D). For each drug, local subnetworks were generated by integrating all shortest paths (length ≤ 3) between the drug targets (pink) and key calcification regulators (dark gray).

TABLE 1 Drug repositioning for the calcification endophenotype module based on network proximity analysis

Drug ID	Drug name	ATC code	Targets	Proximity	*Z*-score	P_{adj}
DB01590	**Everolimus**	L01, L04	MTOR	0	−4.85	.0007
DB06287	**Temsirolimus**	L01	MTOR	0	−4.85	.0007
DB09036	Siltuximab	L04	IL6	0	−4.45	.0047
DB08910	**Pomalidomide**	L04	CRBN, PTGS2, TNF	0.33	−4.03	.0305
DB01169	Arsenic trioxide	L01	CCND1, IKBKB, JUN, MAPK1, MAPK3	0.4	−3.98	.0381
DB11639	Dibotermin alfa (rhBMP-2)	M05	BMPR1A, BMPR2	0	−3.97	.0389

Note: In vitro experimental validation was performed for everolimus, temsirolimus, and pomalidomide (marked in bold).

P_{adj}, Bonferroni-corrected *P* values.

Abbreviation: ATC, anatomical therapeutic chemical.

(20 nmol/L), temsirolimus (10 nmol/L), or pomalidomide (10 μmol/L). Compared to HCSMCs exposed to calcification medium alone, cells treated with these drugs demonstrated a significant reduction in calcification as assessed by Alizarin red staining (Figure 5A). To provide further evidence that the drugs interacted with their respective targets in the network, HCSMCs were exposed to calcification medium in the presence of everolimus, temsirolimus, or pomalidomide for 24 hours. Compared to cells exposed to calcification medium alone, everolimus or temsirolimus decreased phosphorylation of mTOR (0.12 ± 0.03 vs 0.06 ± 0.02 vs 0.06 ± 0.01 arb. units, $P = 0.02$, n = 6) without affecting mTOR expression.

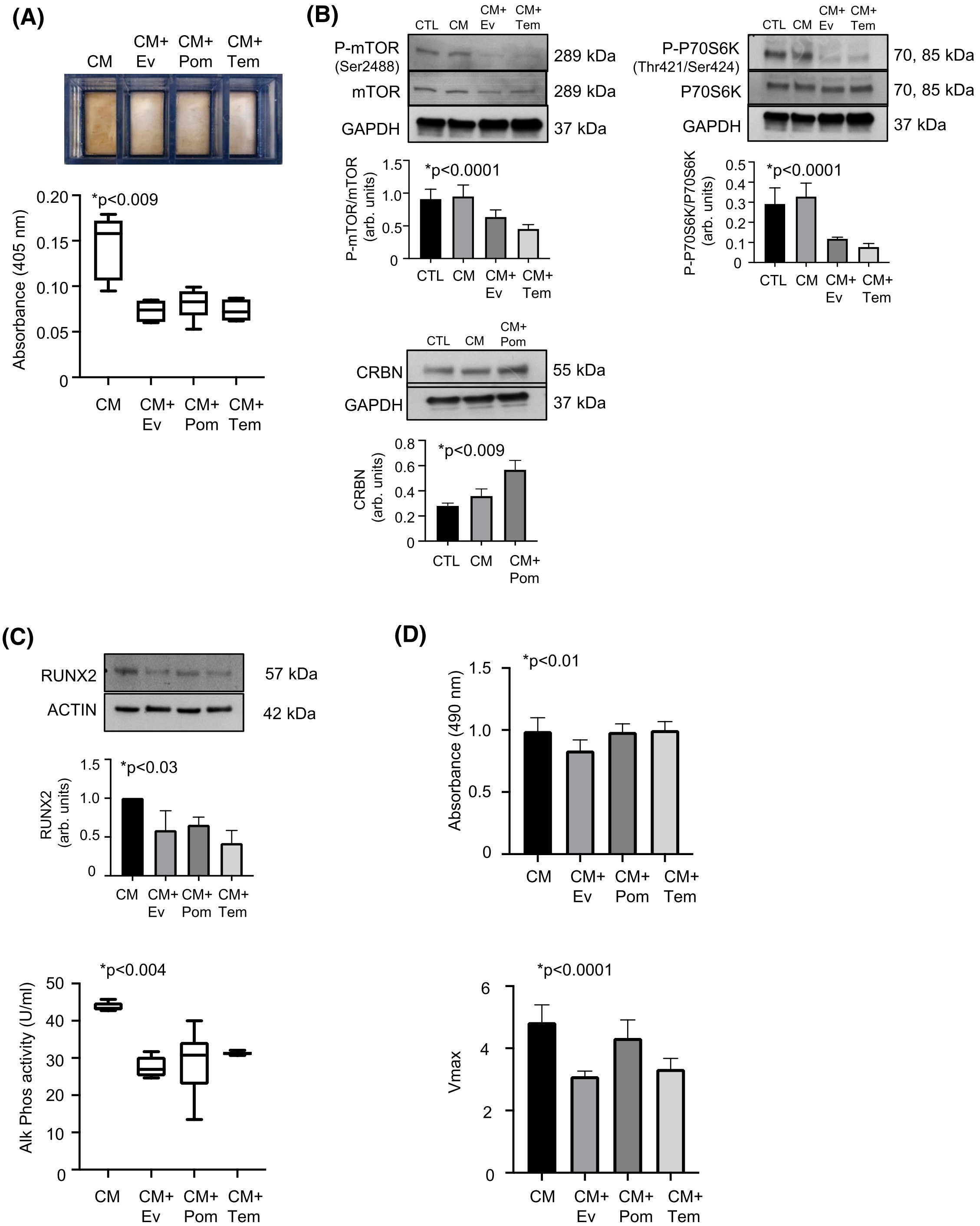

FIGURE 5 Drugs identified by network analysis ameliorate vascular smooth muscle cell calcification. A, Human coronary artery smooth muscle cells (HCSMCs) were treated with everolimus, pomalidomide, or temsirolimus for 10 days. Calcification was assessed visually using Alizarin red staining (*top*) and semiquantitatively (*bottom*) (n = 5). B, Western immunoblotting of HCSMCs exposed to calcification medium and drugs for 24 hours demonstrated that the drugs interacted with their respective network targets. Since everolimus and temsirolimus inhibit mTOR activity, P70S6K activation was also measured as an indicator of effective inhibition (n = 5-6). C, Western immunoblotting of HCSMCs exposed to calcification medium and drugs for 7 days demonstrated a decrease in the expression of the osteoblast transcription factor Runx2 (*top*) (n = 3) and a decrease in alkaline phosphatase activity (*bottom*) (n = 5). D, Cell proliferation (*top*) and apoptosis (*bottom*) were examined in HCSMC exposed to calcification medium and drugs for 10 days to show that observed differences in calcification did not the result from changes in cell number or viability. CTL, control; CM, calcification medium; Ev, everolimus (20 nmol/L); Pom, pomalidomide (10 µmol/L); Tem, temsirolimus (10 nmol/L).

As everolimus and temsirolimus exert their effect by inhibiting mTOR activity, we next examined phosphorylation of P70S6K. Treatment with everolimus or temsirolimus decreased phosphorylation of P70S6K (0.10 ± 0.01 vs 0.03 ± 0.004 vs 0.02 ± 0.002 arb. units, $P < 0.003$, $n = 6$), indicating effective interaction between the drugs and mTOR. Pomalidomide, a derivative of thalidomide, increased the expression of its target protein cereblon (0.20 ± 0.06 vs 0.36 ± 0.08 arb. units, $P < 0.02$, $n = 5$) (Figure 5B).

To provide further evidence that everolimus, pomalidomide, and temsirolimus abrogated transition of HCSMCs to osteoblast-like cells, we examined expression of the osteoblast transcription factor Runx2 in HCSMCs exposed to calcification medium and drugs for 7 days. Compared to untreated HCSMC, treatment with everolimus, pomalidomide, or temsirolimus resulted in a decrease in Runx2 expression (1.0 ± 0.0 vs 0.59 ± 0.15 vs 0.65 ± 0.06 vs 0.42 ± 0.10 arb. units, $P < 0.03$, $n = 3$). This was associated with a decrease in alkaline phosphatase activity (43.8 ± 0.5 vs 27.6 ± 1.1 vs 28.9 ± 3.6 vs 31.3 ± 0.2 U/mL, $P < 0.004$, $n = 4$) (Figure 5C). Next, we examined proliferation and apoptosis in HCSMC exposed to everolimus, pomalidomide, and temsirolimus for 10 days to determine whether the observed effects of these drugs on calcification could be attributed to a decrease in cell number or viability. While everolimus decreased cell proliferation $15.0 \pm 4.5\%$ compared to calcification medium alone, there was no observed difference in HCSMC treated with pomalidomide and temsirolimus (1.0 ± 0.04 vs 0.83 ± 0.04 vs 0.98 ± 0.02 vs 1.0 ± 0.02 arb. units, $P < 0.01$, $n = 8$). Compared to HCSMC exposed to calcification medium alone, treatment with everolimus, pomalidomide, and temsirolimus decreased apoptosis (4.8 ± 0.2 vs 3.1 ± 0.1 vs 4.3 ± 0.2 vs 3.3 ± 0.1 arb. units, $P < 0.0001$, $n = 8$) (Figure 5D). Taken together, these findings indicate that the drugs predicted to target the network are efficacious for the reduction of in vitro HCSMC calcification and affect the relevant in vitro pathways.

4 | DISCUSSION

Cardiovascular calcification is a complex pathological process attributable to several disparate etiologies and associated with many diseases. Identifying effective drugs that prevent or ameliorate ectopic calcification represents an unmet need for preventing the development and progression of cardiovascular diseases. To begin to bridge this gap, we identified the functional calcification endophenotype module (ie, calcificasome) in the human VSMC-specific interactome and compared it with other common endophenotype modules in the PPI network. We found that the calcificasome highly overlaps with the inflammasome, fibrosome, and thrombosome, from which all calcification subendophenotype modules were topologically well defined (clustered) in the PPI network. The finding of overlap and discrete components of the subendophenotype modules further highlights the mechanistic complexity and heterogeneity associated with vascular calcification. We also identified associations between several complex diseases and the calcification process that were previously unrecognized, as well as drugs that target the calcification module with the potential to be repurposed to limit cardiovascular calcification.

Our analyses also identified several significant intermediary genes that may play essential roles in the calcification process by betweenness centrality analysis of the calcification subendophenotype modules. Nuclear factor erythroid-derived 2-like 2 (NFE2L2, also known as NRF2) appears to play a pivotal role in the calcification subendophenotype modules involving inflammation, fibrosis, and thrombosis, confirming prior experimental studies ("positive control" for this network analysis). Several in vitro studies demonstrated that activation of Nrf2 signaling alleviates hyperphosphatemia-induced VSMC calcification by protecting cells from reactive oxygen species (ROS) and downregulating osteogenic transcription factors.[51-53] In contrast, glucose oxidase-mediated osteogenic differentiation and mineralization are inhibited by Nrf2 knockdown in embryonic stem cells.[54] This context-dependent complex behavior of Nrf2 and its relationship to inflammatory-, fibrosis-, and thrombosis-mediated calcification remains incompletely characterized and requires further investigation.

We determined disease-disease associations in terms of the average network distance by curating unbiased human disease genes from GWAS data sets and the OMIM database. As supported by several experimental and clinical studies, we found significant overlap between the calcification subendophenotype modules and those of aortic aneurysm,[8] coronary artery disease,[6] and cardiac arrhythmias.[55] Additionally, ARVD, PCOS, and type 2 DM networks (disease modules) are specifically associated with the pure calcificasome, indicating that putative calcification-related pathways may contribute directly to the pathobiology of those diseases (or vice versa). There is abundant clinical evidence that significant coronary artery and aortic calcification is more prevalent in patients with PCOS or type 2 DM[56-59]; however, the mechanisms of calcification are poorly understood in these disorders. Furthermore, our differential network proximity analysis revealed that the ARVD network is significantly closer to the pure calcificasome than the inflammo-calcificasome or thrombo-calcificasome. Preclinical studies of DSG2-related ARVD mice demonstrate mineralization of mitochondria, which is followed by myocardial calcification and fibro-fatty replacement.[60,61] In contrast, DSP/JUP-related ARVD mice do not develop calcification, likely owing to suppression of the canonical Wnt/β-catenin signaling pathway.[62-64] Our analysis found that the ARVD module is connected to MYC, CSNK2A2, and BMPR1A, which may affect the Wnt/β-catenin pathway or the BMP/

Smad pathway, and provides a plausible link between ARVD and calcification as well as explains the absence of calcification in DSP/JUP-related ARVD mice. The causal relationship between the aforementioned (and other) putative calcification-related pathways in the pathobiology of ARVD remains to be determined.

Our network-based in silico drug repurposing analysis identified several drugs whose targets are more proximal to the calcificasome than that expected by chance. Our experimental findings demonstrated that two rapamycin derivatives (everolimus and temsirolimus) decreased HCSMC calcification as predicted by the network-based drug repurposing analysis. This is not surprising as prior studies have shown that rapamycin (also known as sirolimus), a related drug, is protective in uremic vascular calcification,[65] and rapamycin-mediated downregulation of mTOR activity inhibits smooth muscle cell differentiation into osteoblast-like cells.[66] Recent in vitro and in vivo studies revealed that rapamycin ameliorates CKD/phosphate-induced vascular calcification through upregulation of Klotho.[67] Our data, however, demonstrated further that pomalidomide decreased HCSMC calcification in vitro, a link that has not been established previously. Pomalidomide, a thalidomide derivative, has three targets in the network: cereblon, tumor necrosis factor-α, and cyclooxygenase-2. Of these, we chose to examine cereblon as tumor necrosis factor-α has been implicated previously in vascular calcification[68] and cyclooxygenase-2 was poorly expressed in HCSMCs. Pomalidomide increased cereblon expression in HCSMCs, which is consistent with prior studies that have shown that pomalidomide inhibits ubiquitination and degradation of cereblon in myeloma cell lines.[69] Increased levels of cereblon, in turn, are known to inactivate adenosine monophosphate-activated protein kinase α1, which has been implicated in cardiovascular calcification.[70,71] Thus, we have demonstrated that an integrated network analysis provides new mechanistic insight and novel pharmacological targets, and potentially repositions approved pharmacotherapies for cardiovascular calcification.

In this study, publication or selection bias might contribute to the generation of an incomplete calcification module. Since disease modules and network distance measures are identifiable and reproducible in the setting of data incompleteness,[17] the limited literature information on the calcification process would not significantly affect overall results. We used pulmonary arterial SMC to construct the VSMC-interactome, which may limit our ability to explain fully coronary artery calcification (although calcification of the pulmonary arteries in severe pulmonary hypertension is well recognized).

ACKNOWLEDGMENTS

We thank Stephanie Tribuna for expert technical assistance. This work as supported in part by NIH grants HG007690, HL108630, and HL119145, and AHA grant D700382 to J. Loscalzo, and NIH grant HL125215 and AHA grant 19AIML34980000 to J. Leopold.

CONFLICT OF INTEREST

J. Loscalzo is the Scientific co-founder of Scipher Medicine, Inc., a company that applies the principles of network medicine to diagnostics and therapeutics.
J-S Song, R. Wang, and J. A. Leopold have no conflicts of interest to declare.

AUTHOR CONTRIBUTIONS

Designed, performed, analyzed data, and wrote the paper: J.-S. Song
Contributed new analytic tools, and analyzed the data; critically reviewed the paper: R.-S. Wang
Performed research, contributed new reagents, analytic tools, and critically reviewed and wrote newer sections of the paper: J. A. Leopold
Oversaw the design of the research, contributed reagents and analytic tools, analyzed the data, and critically reviewed and edited the paper: J. Loscalzo

REFERENCES

1. Demer LL, Tintut Y. Vascular calcification: pathobiology of a multifaceted disease. *Circulation*. 2008;117:2938-2948.
2. Budoff MJ, Hokanson JE, Nasir K, et al. Progression of coronary artery calcium predicts all-cause mortality. *JACC: Cardiovasc Imag*. 2010;3:1229-1236.
3. Budoff MJ, McClelland RL, Nasir K, et al. Cardiovascular events with absent or minimal coronary calcification: The Multi-Ethnic Study of Atherosclerosis (MESA). *Am Heart J*. 2009;158:554-561.
4. Folsom AR, Kronmal RA, Detrano RC, et al. Coronary artery calcification compared with carotid intima-media thickness in the prediction of cardiovascular disease incidence: the multi-ethnic study of atherosclerosis (MESA). *Arch Intern Med*. 2008;168:1333-1339.
5. Johnson RC, Leopold JA, Loscalzo J. Vascular calcification: pathobiological mechanisms and clinical implications. *Circ Res*. 2006;99:1044-1059.
6. Doherty TM, Asotra K, Fitzpatrick LA, et al. Calcification in atherosclerosis: Bone biology and chronic inflammation at the arterial crossroads. *Proc Natl Acad Sci USA*. 2003;100:11201-11206.
7. Rajamannan NM, Evans FJ, Aikawa E, et al. Calcific aortic valve disease: not simply a degenerative process: a review and agenda for research from the National Heart and Lung and Blood Institute Aortic Stenosis Working Group. Executive summary: Calcific aortic valve disease-2011 update. *Circulation*. 2011;124:1783-1791.
8. Jayalath RW, Mangan SH, Golledge J. Aortic calcification. *Eur J Vasc Endovasc Surg*. 2005;30:476-488.
9. Loscalzo J, Kohane I, Barabasi AL. Human disease classification in the postgenomic era: a complex systems approach to human pathobiology. *Mol Syst Biol*. 2007;3:124.
10. Fox EA, Kahn SR. The relationship between inflammation and venous thrombosis. A systematic review of clinical studies. *Thromb Haemost*. 2005;94:362-365.
11. Libby P, Simon DI. Inflammation and thrombosis: the clot thickens. *Circulation*. 2001;103:1718-1720.

12. Rogers MA, Aikawa E. Cardiovascular calcification: artificial intelligence and big data accelerate mechanistic discovery. *Nat Rev Cardiol*. 2019;16:261-274.
13. Ghiassian SD, Menche J, Chasman DI, et al. Endophenotype network models: common core of complex diseases. *Sci Rep*. 2016;6:27414.
14. Cheng F, Desai RJ, Handy DE, et al. Network-based approach to prediction and population-based validation of in silico drug repurposing. *Nat Commun*. 2018;9:2691.
15. Guney E, Menche J, Vidal M, Barabasi AL. Network-based in silico drug efficacy screening. *Nat Commun*. 2016;7:10331.
16. Barabási A-L, Gulbahce N, Loscalzo J. Network medicine: a network-based approach to human disease. *Nat Rev. Genet*. 2011;12:56-68.
17. Menche J, Sharma A, Kitsak M, et al. Disease networks. Uncovering disease-disease relationships through the incomplete interactome. *Science*. 2015;347:1257601.
18. Goh K-I, Cusick ME, Valle D, Childs B, Vidal M, Barabási A-L. The human disease network. *Proc Natl Acad Sci USA*. 2007;104:8685-8690.
19. Xu J, Li Y. Discovering disease-genes by topological features in human protein–protein interaction network. *Bioinformatics*. 2006;22:2800-2805.
20. Zhou X, Menche J, Barabási A-L, Sharma A. Human symptoms–disease network. *Nat Commun*. 2014;5:4212.
21. Koschutzki D, Schreiber F. Centrality analysis methods for biological networks and their application to gene regulatory networks. *Gene Regul Syst Bio*. 2008;2:193-201.
22. Cheng F, Lu W, Liu C, et al. A genome-wide positioning systems network algorithm for in silico drug repurposing. *Nat Commun*. 2019;10:3476.
23. Zhou Y, Hou Y, Shen J, Huang Y, Martin W, Cheng F. Network-based drug repurposing for novel coronavirus 2019-nCoV/SARS-CoV-2. *Cell Discov*. 2020;6:14.
24. Gysi DM, Valle ÍD, Zitnik M, et al.Network medicine framework for identifying drug repurposing opportunities for covid-19. 2020; arXiv preprint arXiv:2004.07229.
25. Cheng F, Kovacs IA, Barabasi AL. Network-based prediction of drug combinations. *Nat Commun*. 2019;10:1197.
26. Rual JF, Venkatesan K, Hao T, et al. Towards a proteome-scale map of the human protein-protein interaction network. *Nature*. 2005;437:1173-1178.
27. Venkatesan K, Rual JF, Vazquez A, et al. An empirical framework for binary interactome mapping. *Nat Meth*. 2009;6:83-90.
28. Yu H, Tardivo L, Tam S, et al. Next-generation sequencing to generate interactome datasets. *Nat Meth*. 2011;8:478-480.
29. Rolland T, Tasan M, Charloteaux B, et al. A proteome-scale map of the human interactome network. *Cell*. 2014;159:1212-1226.
30. Yang X, Coulombe-Huntington J, Kang S, et al. Widespread expansion of protein interaction capabilities by alternative splicing. *Cell*. 2016;164:805-817.
31. Stelzl U, Worm U, Lalowski M, et al. A human protein-protein interaction network: a resource for annotating the proteome. *Cell*. 2005;122:957-968.
32. Yachie N, Petsalaki E, Mellor JC, et al. Pooled-matrix protein interaction screens using Barcode Fusion Genetics. *Mol Syst Biol*. 2016;12:863.
33. Ewing RM, Chu P, Elisma F, et al. Large-scale mapping of human protein-protein interactions by mass spectrometry. *Mol Syst Biol*. 2007;3:89.
34. Havugimana PC, Hart GT, Nepusz T, et al. A census of human soluble protein complexes. *Cell*. 2012;150:1068-1081.
35. Kristensen AR, Gsponer J, Foster LJ. A high-throughput approach for measuring temporal changes in the interactome. *Nat Meth*. 2012;9:907-909.
36. Huttlin EL, Ting L, Bruckner RJ, et al. The BioPlex network: a systematic exploration of the human interactome. *Cell*. 2015;162:425-440.
37. Wan C, Borgeson B, Phanse S, et al. Panorama of ancient metazoan macromolecular complexes. *Nature*. 2015;525:339-344.
38. Hein MY, Hubner NC, Poser I, et al. A human interactome in three quantitative dimensions organized by stoichiometries and abundances. *Cell*. 2015;163:712-723.
39. Huttlin EL, Bruckner RJ, Paulo JA, et al. Architecture of the human interactome defines protein communities and disease networks. *Nature*. 2017;545:505-509.
40. Hornbeck PV, Zhang B, Murray B, Kornhauser JM, Latham V, Skrzypek E. PhosphoSitePlus, 2014: mutations, PTMs and recalibrations. *Nucleic Acids Res*. 2015;43:D512-D520.
41. Newman RH, Hu J, Rho HS, et al. Construction of human activity-based phosphorylation networks. *Mol Syst Biol*. 2013;9:655.
42. Vinayagam A, Stelzl U, Foulle R, et al. A directed protein interaction network for investigating intracellular signal transduction. *Sci Signal*. 2011;4:rs8.
43. Turei D, Korcsmaros T, Saez-Rodriguez J. OmniPath: guidelines and gateway for literature-curated signaling pathway resources. *Nat Methods*. 2016;13:966-967.
44. Wang RS, Oldham WM, Loscalzo J. Network-based association of hypoxia-responsive genes with cardiovascular diseases. *New J Phys*. 2014;16:105014.
45. Schlotter F, Halu A, Goto S, et al. Spatiotemporal multi-omics mapping generates a molecular atlas of the aortic valve and reveals networks driving disease. *Circulation*. 2018;138:377-393.
46. Zeng Z, dos Sarbassov D, Samudio IJ, et al. Rapamycin derivatives reduce mTORC2 signaling and inhibit AKT activation in AML. *Blood*. 2007;109:3509-3512.
47. Lebwohl D, Anak O, Sahmoud T, et al. Development of everolimus, a novel oral mTOR inhibitor, across a spectrum of diseases. *Ann N Y Acad Sci*. 2013;1291:14-32.
48. Lopez-Girona A, Mendy D, Ito T, et al. Cereblon is a direct protein target for immunomodulatory and antiproliferative activities of lenalidomide and pomalidomide. *Leukemia*. 2012;26:2326-2335.
49. Balcells M, Martorell J, Olive C, et al. Smooth muscle cells orchestrate the endothelial cell response to flow and injury. *Circulation*. 2010;121:2192-2199.
50. Zickler D, Luecht C, Willy K, et al. Tumour necrosis factor-alpha in uraemic serum promotes osteoblastic transition and calcification of vascular smooth muscle cells via extracellular signal-regulated kinases and activator protein 1/c-FOS-mediated induction of interleukin 6 expression. *Nephrol Dial Transplant*. 2018;33:574-585.
51. Yao L, Wang J, Tian BY, Xu TH, Sheng ZT. Activation of the Nrf2-ARE signaling pathway prevents hyperphosphatemia-induced vascular calcification by inducing autophagy in renal vascular smooth muscle cells. *J Cell Biochem*. 2017;118:4708-4715.
52. Ganesan AN, Kuklik P, Gharaviri A, et al. Origin and characteristics of high Shannon entropy at the pivot of locally stable rotors: insights from computational simulation. *PLoS One*. 2014;9:e110662.
53. Wei R, Enaka M, Muragaki Y. Activation of KEAP1/NRF2/P62 signaling alleviates high phosphate-induced calcification of

vascular smooth muscle cells by suppressing reactive oxygen species production. *Sci Rep*. 2019;9:10366.
54. Sim HJ, Kim JH, Kook SH, Lee SY, Lee JC. Glucose oxidase facilitates osteogenic differentiation and mineralization of embryonic stem cells through the activation of Nrf2 and ERK signal transduction pathways. *Mol Cell Biochem*. 2016;419:157-163.
55. Alyesh DM, Siontis KC, Dabbagh GS, et al. Postinfarction myocardial calcifications on cardiac computed tomography. *Circulation: Arrhythm Electrophysiol*. 2019;12:e007023.
56. Talbott EO, Zborowski JV, Rager JR, Boudreaux MY, Edmundowicz DA, Guzick DS. Evidence for an association between metabolic cardiovascular syndrome and coronary and aortic calcification among women with polycystic ovary syndrome. *J Clin Endocrinol Metab*. 2004;89:5454-5461.
57. Calderon-Margalit R, Siscovick D, Merkin Sharon S, et al. Prospective association of polycystic ovary syndrome with coronary artery calcification and carotid-intima-media thickness. *Arterioscler Thromb Vasc Biol*. 2014;34:2688-2694.
58. Meigs JB, Larson MG, D'Agostino RB, et al. Coronary artery calcification in type 2 diabetes and insulin resistance. The Framingham Offspring Study. *Diabetes Care*. 2002;25:1313-1319.
59. Liabeuf S, Olivier B, Vemeer C, et al. Vascular calcification in patients with type 2 diabetes: the involvement of matrix Gla protein. *Cardiovasc Diabetol*. 2014;13:85.
60. Pilichou K, Remme CA, Basso C, et al. Myocyte necrosis underlies progressive myocardial dystrophy in mouse dsg2-related arrhythmogenic right ventricular cardiomyopathy. *J Exp Med*. 2009;206:1787-1802.
61. Krusche CA, Holthofer B, Hofe V, et al. Desmoglein 2 mutant mice develop cardiac fibrosis and dilation. *Basic Res Cardiol*. 2011;106:617-633.
62. Garcia-Gras E, Lombardi R, Giocondo MJ, et al. Suppression of canonical Wnt/β-catenin signaling by nuclear plakoglobin recapitulates phenotype of arrhythmogenic right ventricular cardiomyopathy. *J Clin Invest*. 2006;116:2012-2021.
63. Yang Z, Bowles NE, Scherer SE, et al. Desmosomal dysfunction due to mutations in desmoplakin causes arrhythmogenic right ventricular dysplasia/cardiomyopathy. *Circ Res*. 2006;99:646-655.
64. Li J, Swope D, Raess N, Cheng L, Muller EJ, Radice GL. Cardiac tissue-restricted deletion of plakoglobin results in progressive cardiomyopathy and activation of {beta}-catenin signaling. *Mol Cell Biol*. 2011;31:1134-1144.
65. Frauscher B, Kirsch AH, Schabhüttl C, et al. Autophagy protects from uremic vascular media calcification. *Front Immunol*. 2018;14:1866.
66. Zhan JK, Wang YJ, Wang Y, et al. The mammalian target of rapamycin signalling pathway is involved in osteoblastic differentiation of vascular smooth muscle cells. *Can J Cardiol*. 2014;30:568-575.
67. Zhao Y, Zhao MM, Cai Y, et al. Mammalian target of rapamycin signaling inhibition ameliorates vascular calcification via Klotho upregulation. *Kidney Int*. 2015;88:711-721.
68. Hénaut L, Sanchez-Nino MD, Aldamiz-Echevarría Castillo G, Sanz AB, Ortiz A. Targeting local vascular and systemic consequences of inflammation on vascular and cardiac valve calcification. *Expert Opin Ther Targets*. 2016;20:89-105.
69. Liu Y, Huang X, He X, et al. A novel effect of thalidomide and its analogs: suppression of cereblon ubiquitination enhances ubiquitin ligase function. *FASEB J*. 2015;29:4829-4839.
70. Lee KM, Jo S, Kim H, Lee J, Park CS. Functional modulation of AMP-activated protein kinase by cereblon. *Biochim Biophys Acta*. 2011;1813:448-455.
71. Cai Z, Ding Y, Zhang M, et al. Ablation of adenosine monophosphate-activated protein kinase α1 in vascular smooth muscle cells promotes diet-induced atherosclerotic calcification in vivo. *Circ Res*. 2016;119:422-433.

SUPPORTING INFORMATION

Additional Supporting Information may be found online in the Supporting Information section.

How to cite this article: Song J-S, Wang R-S, Leopold JA, Loscalzo J. Network determinants of cardiovascular calcification and repositioned drug treatments. *The FASEB Journal*. 2020;34:11087–11100. https://doi.org/10.1096/fj.202001062R